Available online at www.sciencedirect.com
SCIENCE DIRECT®
Journal of Photochemistry and Photobiology A: Chemistry 161 (2004) 105–110
Journal of Photochemistry and Photobiology A:Chemistry
www.elsevier.com/locate/jphotochem

Photovoltaic characteristics of dye-sensitized surface-modified nanocrystalline SnO_2 solar cells

Nam-Gyu Park*, Man Gu Kang, Kwang Sun Ryu, Kwang Man Kim, Soon Ho Chang

Basic Research Laboratory, Electronics and Telecommunications Research Institute (ETRI), Daejeon 305-350, South Korea

Received 19 March 2003; received in revised form 17 May 2003; accepted 19 May 2003

Abstract

Zinc-modified nanocrystalline SnO_2 electrodes are prepared by chemical treatment of the commercial SnO_2 colloid with zinc acetate and their thickness effects on photovoltaic characteristics are investigated. Open-circuit voltage (V_{oc}) and fill factor increase with increasing zinc concentration, while short-circuit photocurrent (J_{sc}) decreases. The normalized incident photon-to-current conversion efficiency (IPCE) shows that increase of zinc concentration utilizes long wavelength light. Concerning the conversion efficiency, optimal concentration within the present experiment is found to be 10 mol.% Zn^{2+} with respect to Sn^{4+}. As increasing thickness of the films based on 10 mol.% zinc-modified SnO_2 ranging from 0.76 to 8.12 μm, J_{sc} increases, reaches maximum and then decreases without change in V_{oc}. The highest conversion efficiency of about 3.4% is achieved under 1 sun of AM 1.5 irradiation for the ∼6.3 μm-thick 10 mol.% zinc-modified SnO_2 film with J_{sc} of 9.09 mA/cm^2, V_{oc} 600 mV and fill factor 62%.

Keywords: Dye-sensitized; Tin oxide; Surface modification; Nanocrystalline; Thickness effect

1. Introduction

Since the report on high-efficiency and low-cost solar cells based on dye-sensitized nanocrystalline TiO_2 [1], dye-sensitized solar cells (DSSCs) have become the most promising alternative to conventional silicon-based photovoltaic devices [2]. DSSC is composed of a few micrometer-thick film consisting nanocrystalline oxide covered with monolayer of Ru-bipyridyl-based charge-transfer dye, a redox electrolyte and a platinum metal electrode. Thanks to the large internal surface area of the nanoparticle film, the light-harvesting efficiency of the dye monolayer is high, which means that one of the key components of DSSCs is the nanocrystalline semiconductor electrode. So far the highest energy conversion efficiencies have been achieved with nanocrystalline anatase TiO_2 [3,4]. Other materials, such as SnO_2 [5–8], ZnO [9–14], and Nb_2O_5 [15], have been tested as supports for dye molecules and electron transporting media, but their energy conversion efficiencies turn out to be mostly as low as 1–2%. For the case of SnO_2, it has been reported that almost all the excited dye molecules inject electrons on SnO_2 within ∼150 ps [16], suggesting electron injection process does not seem to be responsible for considerably low energy conversion efficiency. The poor performance of the SnO_2-based solar cells is thus probably related to the intrinsic property of SnO_2 such as 0.4 V more positive conduction band potential than TiO_2 [17], which lowers open-circuit voltage (V_{oc}) and may have influence on electron loss from conduction band to electrolyte via surface states because of decreased potential difference between surface states and redox electrolyte [18,19]. Based on the energy levels of each component in dye-sensitized solar cell, it is expected that the maximum open-circuit voltage is theoretically 0.5 V from the potential difference between the potential of the conduction band of SnO_2 (−0.3 V versus SCE) and the I^-/I_3^- redox potential (0.2 V versus SCE).

Recently, energy conversion efficiencies of nanocrystalline SnO_2-based solar cell have been significantly improved by surface "*nanopainting*" technique with a thin layer of MgO [20], ZnO [21], TiO_2 [22], and several insulating oxides [23]. This approach increases both short-circuit photocurrent (J_{sc}) and open-circuit voltage (V_{oc}), especially a large increase in V_{oc} has been achieved. In addition, it is pointed out that surface-modified SnO_2 can offer the advantage of better long-term stability than TiO_2 because of low sensitivity to UV degradation due to larger band gap [23]. Although poor performance of bare SnO_2 has been overcome by surface modification, optimization study such as film thickness effect has not been yet performed.

* Corresponding author. Tel.: +82-42-860-5680; fax: +82-42-860-6836.
E-mail address: npark@etri.re.kr (N.-G. Park).

1010-6030/$ – see front matter © 2004 Elsevier B.V. All rights reserved.
doi:10.1016/S1010-6030(03)00280-6

In this work, we report on photovoltaic characteristics of dye-sensitized solar cells based on nanocrystalline SnO_2 modified with zinc acetate, where we investigate effects of zinc acetate concentration and film thickness on *J–V* and incident photon-to-current conversion efficiency (IPCE).

2. Experimental

2.1. Preparation of surface-modified SnO_2 films

Commercially available colloidal SnO_2 (Alfa Aesar, 15 wt.% in H_2O) was used and its surface was modified using $Zn(CH_3COO)_2{\cdot}2H_2O$ (Aldrich) as follows. Five grams of 15% SnO_2 colloidal solution (containing 0.75 g of SnO_2) was taken and poured into the bottle with magnetic stirrer. Polyethylene glycol of 0.3 g (Fluka, MW 20,000) was added to the colloidal and stirred, followed by adding 54.6 mg of zinc acetate (10 mol.% of Zn^{2+} with respect to Sn^{4+}) or 0.11 g (20 mol.% Zn^{2+}). After addition of zinc acetate into the basic SnO_2 colloidal solution, gelation takes place immediately, which makes mixing stop. 0.8 ml of 0.5 M acetic acid aqueous solution and 0.5 ml of methanol were then added to dilute and keep mixing the mixture. Finally, 0.15 g of poly(ethylene oxide) (Aldrich, MW 80,000) was added to make viscous coating slurry.

The resulting slurry was coated with a doctor blade onto a transparent electrical conducting glass (Libbey–Owens–Ford; F-doped SnO_2 overlayer; 80% transmittance in the visible; 5% haze; 8 Ω/□), dried at 80 °C, and subsequently heated in air for 1 h at 500 °C. The thickness of the Zn-coated SnO_2 films was varied from 0.8 to 8.1 μm and measured with a Tencor Alpha-Step 500 profiler.

2.2. Photosensitization and solar cell assembly

The resulting surface-modified SnO_2 films were immersed in absolute ethanol containing 3×10^{-4} M $Ru[LL'(NCS)_2]$ (L = 2,2′-bipyridyl-4,4′-dicarboxylic acid, L′ = 2,2′-bipyridyl-4,4′-ditetrabutylammoniumcarboxylate; Solaronix) for 24 h at room temperature. The dye-covered electrodes were then rinsed with absolute ethanol and dried under a N_2 stream. To minimize rehydration of nanocrystalline films from moisture in the ambient air, the electrodes were immersed in the dye solution while they were still warm (100 °C) from the annealing step. Pt counter electrodes were prepared by spreading a drop of 5 mM hexachloroplatinic acid (Fluka, purum) in 2-propanol on the conducting glass followed by heating at 400 °C for 30 min in air. The Pt electrode was placed over the dye-coated electrode, and the edges of the cell were sealed with 0.5-mm-wide strips of 30-μm-thick Surlyn (Dupont, grade 1702). Sealing was accomplished by pressing the two electrodes together at a pressure of 200 kPa/cm^2 and a temperature of about 110 °C within a few seconds. The redox electrolyte consisted of 0.8 M 1,2-dimethyl-3-hexyl-imidazolium iodide (C6DMI) and 40 mM I_2 in acetonitrile was introduced into the cell through one of two small holes drilled in the counter electrode. The holes were then covered and sealed with small squares of microscope objective glass and Surlyn.

2.3. Characterizations

X-ray diffraction (XRD) data were collected using an X-ray diffractometer (Philips PW3040/60 X'Pert PRO) in the 2θ ranging from 20 to 60° with Cu Kα radiation (λ = 1.5406 Å) operated at 30 mA and 40 kV. The film morphology was investigated by a field-emission scanning electron microscope (FE-SEM) (Philips XL30SFEG). J_{sc} and V_{oc} were measured using a Keithley Model 2400 source measure unit. A 1000 W Xenon lamp (Oriel, 91193) served as a light source. The light was homogeneous up to 8 in. × 8 in., and its intensity (or radiant power) was adjusted with a Si solar cell (Fraunhofer Institute for Solar Energy System; Mono-Si + KG filter; Certificate No. C-ISE269) for approximating 1 sun light intensity (100 mW/cm^2) that was double-checked with a NREL-calibrated Si solar cell (PV Measurements Inc.). IPCE was measured as a function of wavelength from 360 to 800 nm using a specially designed IPCE system for dye-sensitized photoelectrochemical cell (PV Measurement Inc.) equipped with halogen source as monochromatic light and a broadband bias light for approximating 1 sun light intensity. Calibration was performed using a silicon reference photodiode (G587), where calibration was transferred from G425 (a NIST-calibrated photodiode) to G587 by PV Measurements Inc. The IPCE values for DSSCs are collected at the low chopping speed of 5 Hz.

3. Results and discussion

Fig. 1 shows XRD patterns of unmodified and Zn-modified SnO_2 films annealed at 500 °C for 1 h. No presence of the isolated ZnO phase is observed upto 20% zinc modification. All the peaks are indexed to be cassiterite SnO_2 phase with broad feature of full-width at half-maximum (FWHM), indicating very small SnO_2 particle size. The crystalline particle size D is also estimated from the X-ray (1 0 1) diffraction peak using the Scherrer equation [24], $D = 0.9\lambda/\beta\cos\theta$, where λ is the wavelength of the X-ray source, β the FWHM and θ is the Bragg angle in the diffraction pattern. The particle size of unmodified SnO_2 is estimated to be about 7.92 nm from the values of λ = 0.15406 nm, 2θ = 33.78° and $\beta = 1.05° = 2\pi \times (1.05°/360°) = 0.0183$ (cf. the as-received Alfa Aesar SnO_2 particle is estimated to be 4.15 nm that is consistent with the previous report [25]). Upon surface treatment with zinc acetate, FWHM increases (see inset in Fig. 1) to β = 1.42 and 1.53° for 10 and 20 mol.% Zn, respectively, resulting in decreased particle size of 5.85 and 5.43 nm.

Fig. 2 shows FE-SEM micrographs of unmodified and Zn-modified SnO_2 films, where the thickness of the 500 °C,

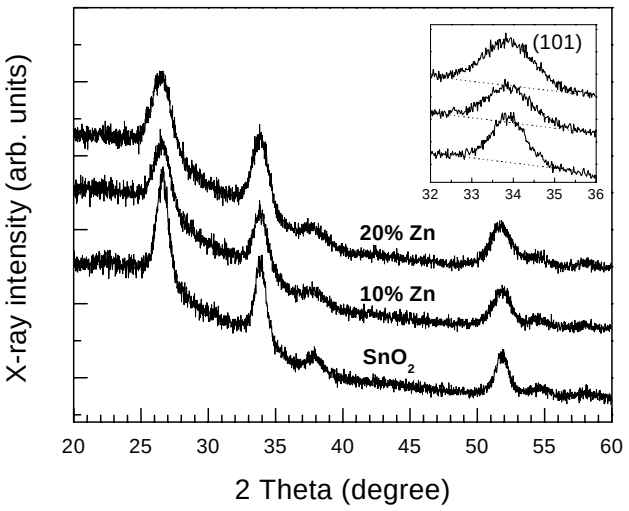

Fig. 1. X-ray diffraction patterns of unmodified SnO_2, 10 and 20 mol.% Zn-modified SnO_2 films annealed 500 °C for 1 h. Inset shows the corresponding (1 0 1) peak.

1 h-annealed films were estimated to be 1.7 ± 0.05 μm. All the films exhibit aggregates, which might be formed during acidification of the basic mother colloidal solution by addition of zinc acetate, associated with undergoing the point of zero charge (pzc) of SnO_2 at pH 4–5 [26]. With increasing the zinc acetate concentration, individual particle size slightly decreases from ~14 to 10, and to ~8 nm upon adding 10 and 20 mol.% Zn^{2+} ions, respectively, indicating Zn^{2+} ions act as an inhibitor against particle growth from the fact that the surface-coated oxide layers stabilize SnO_2 against particle growth [27,28]. Compared with the particle size estimated from XRD, a slight larger particle observed from SEM is due to gold coating for SEM measurement.

Fig. 3 shows the optical micrographs of dye-sensitized unmodified and zinc-modified nanocrystalline SnO_2 electrodes. The coloration of zinc-modified SnO_2 is much stronger than unmodified one and the red color becomes intense as increasing zinc concentration, which is in relation with the decreased particle size and/or the higher pzc of zinc oxide (pH 9) than that of tin oxide (pH 4–5) [23].

Photocurrent–voltage and dark current–voltage characteristics of unmodified SnO_2 and Zn-modified SnO_2 electrodes are compared in Fig. 4. Contrary to the stronger coloration by Zn modification, photocurrent density decreases with increasing zinc concentration from 5.76 (bare SnO_2) to 4.22 (10% Zn) and to 3.33 mA/cm^2 (20% Zn). Open-circuit voltages, however, increase significantly from 0.445 to 0.610 and to 0.635 V together with increase in fill factors from 0.49 to 0.66 and to 0.67. Consequently, conversion efficiency increases from 1.26 to 1.70, and to 1.46% upon 10 and 20 mol.% Zn modification, respectively. It has been observed that surface treatment usually induces an increase of V_{oc} regardless of surface-coated materials and materials to be coated [21,23,29]. The gradual decrease in J_{sc} after zinc modification might be due to a large increase in V_{oc}, presumably associated with change in surface conduction band position. It cannot be also ruled out that J_{sc} and V_{oc} might be influenced by addition of acetic acid alone even in the absence of zinc acetate since the colloidal tin oxide is basic. The addition of acetic acid to the basic tin oxide colloid is likely to cause shift in conduction band position and increase in dye adsorption, which might account for relatively high J_{sc} and low V_{oc}. The dark current–voltage curves in Fig. 4 show that at each given potential Zn-modified SnO_2 electrodes exhibit lower dark current than unmodified SnO_2, suggesting a decrease of the electron recombination rate in relation to the increased V_{oc}. Lowering dark current is also observed when the SnO_2 surface is modified with thin layer of several insulating materials other than zinc oxide [22,23].

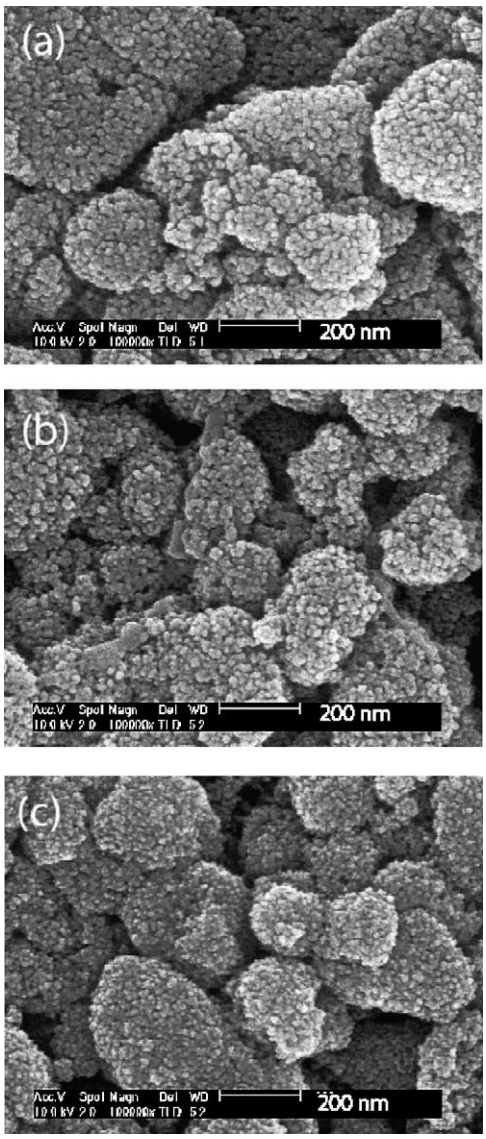

Fig. 2. Scanning electron micrographs of (a) SnO_2, (b) 10 mol.% Zn-modified SnO_2 and (c) 20 mol.% Zn-modified SnO_2 films annealed at 500 °C for 1 h.

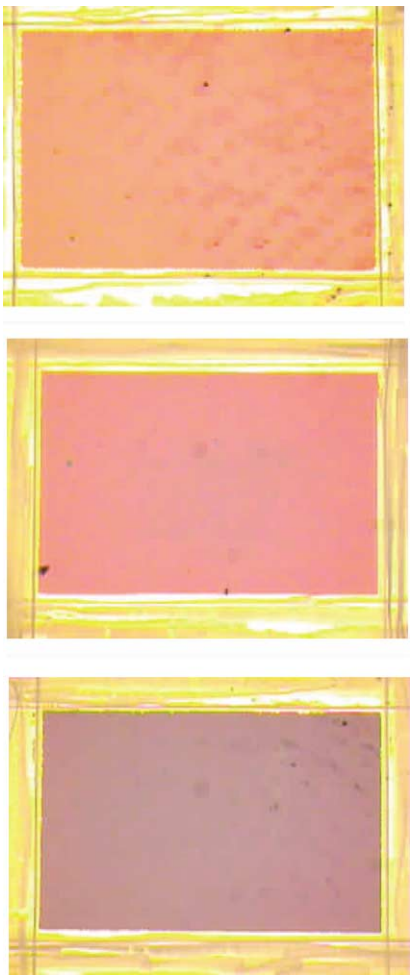

Fig. 3. Color of dye-sensitized (a) SnO_2 film, (b) 10 mol.% Zn- modified SnO_2 film and (c) 20 mol.% Zn-modified SnO_2 film, showing that red color becomes intensely as increasing Zn concentration.

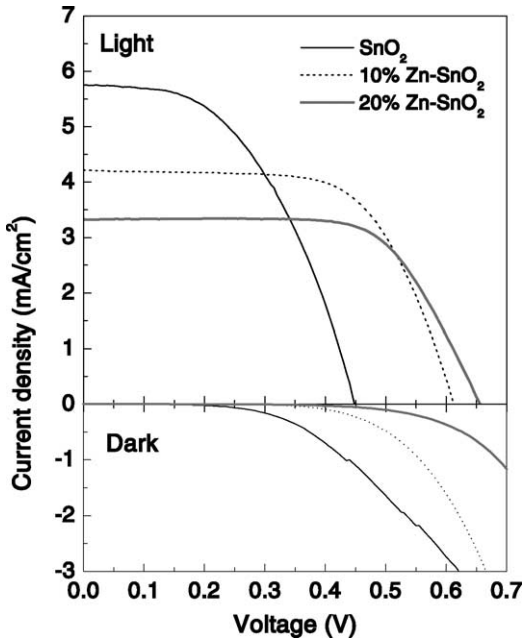

Fig. 4. Photocurrent–voltage and dark current–voltage curves of dye-sensitized unmodified and Zn-modified nanocrystalline SnO_2 electrodes in acetonitrile containing 1,2-dimethyl-3-hexyl-imidazolium iodide (0.8 M) and iodine (40 mM). The radiant power is 100 mW/cm^2.

Fig. 5a displays the IPCE as a function of wavelength measured at short circuit with bias light; no correction was made for reflection losses from the cell. Fig. 5b shows the same IPCE data normalized to the intensity of the 520 nm peak. Following the same trend observed in *J–V* curves, the absolute IPCE values decreases with increasing zinc concentration. It is interesting to see the normalized IPCE spectra that at the same thickness surface modification gives relatively high IPCE in the both short (400–500 nm) and long (600–700 nm) spectral regions, indicating that light absorption by iodide species (I_3^-) in the electrolyte is accentuated in the short wavelength region and the red light is more effectively utilized by surface modification.

Film thickness effect on *J–V* characteristics is investigated for the 10 mol.% Zn-modified SnO_2 electrodes. Fig. 6a and Table 1 show the *J–V* characteristics as a function of film thickness. With increasing film thickness, J_{sc} increases, reaches maximum and then decreases without any significant change in V_{oc}. As a result, the highest conversion efficiency of 3.38% is obtained for the 6.28 μm-thick film (Fig. 6b). Compared with the reported efficiency of 5.2% with $J_{sc} = 11.2$ mA/cm^2 for the 8 μm-thick Zn-modified SnO_2 film with the light scattering SnO_2 (~140 nm) particle [23], the cell performance of the present sample is evaluated to be as good as the reported sample when taking into account thinner film thickness and absence of light-scattering particles.

The IPCE values in Fig. 7a shows the same trend observed in photocurrent change with film thickness in Fig. 6a. The highest IPCE of about 55% is achieved for the 6.28 μm-thick 10 mol.% Zn-modified SnO_2 film. Increasing film thickness improves apparently the conversion efficiency of long wavelength light (Fig. 7b), indicating the thicker films utilize more red light.

Table 1
Effect of film thickness on photocurrent–voltage (*J–V*) characteristics of 10 mol.% Zn-modified SnO_2 electrodes sensitized with Ru[LL′(NCS)$_2$][a,b]

Thickness (μm)	J_{sc} (mA/cm^2)	V_{oc} (V)	FF	Efficiency (%)	Cell area (cm^2)[c]
0.76	2.57	0.59	0.61	0.92	0.2137
1.65	4.18	0.59	0.58	1.43	0.2056
2.82	5.28	0.58	0.59	1.80	0.2206
6.28	9.09	0.60	0.62	3.38	0.2209
8.12	8.56	0.59	0.65	3.28	0.2269

[a] Radiant power: 100 mW/cm^2 (AM 1.5).
[b] Redox electrolyte: 0.8 M 1,2-dimethyl-3-hexyl-immidazolium iodide and 40 mM I_2 in acetonitrile.
[c] Dye-sensitized TiO_2 film area.

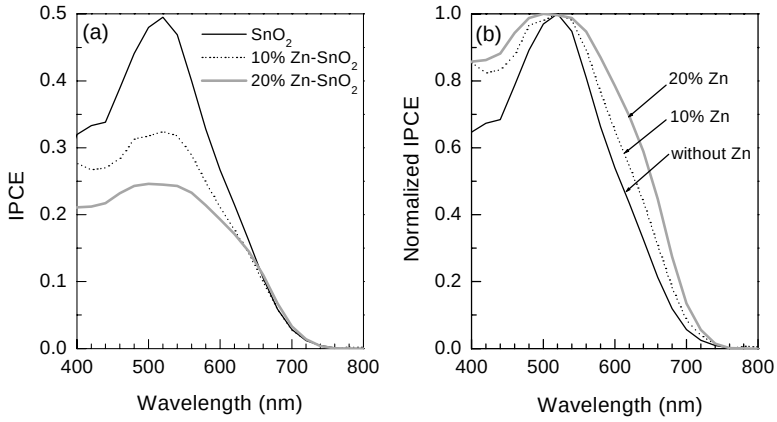

Fig. 5. Dependence of the (a) absolute and (b) normalized values of the IPCE on wavelength for dye-sensitized unmodified and Zn-modified nanocrystalline SnO_2 electrodes. The redox electrolyte contained 1,2-dimethyl-3-hexyl imidazolium iodide (0.8 M) and iodine (40 mM) in acetonitrile. No correction was made for reflection losses.

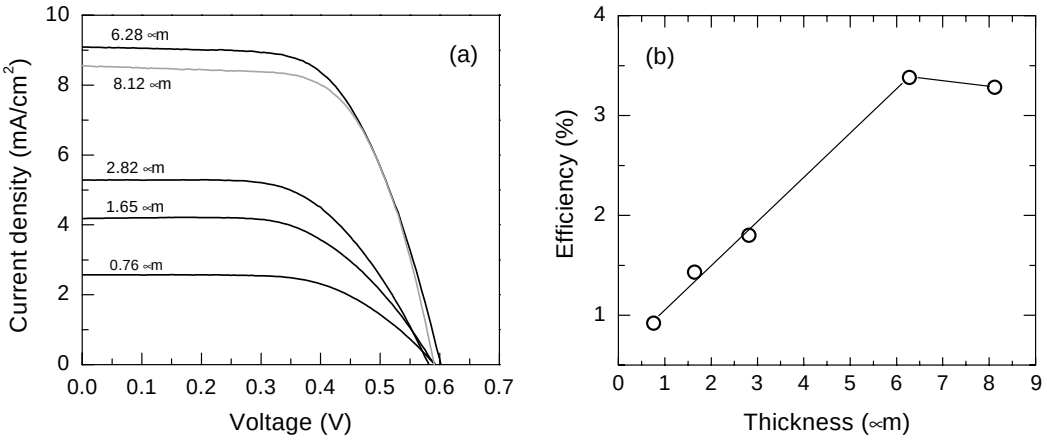

Fig. 6. Dependence of (a) photocurrent–voltage and (b) overall energy conversion efficiency on film thickness of dye-sensitized 10 mol.% Zn-modified nanocrystalline SnO_2 electrodes. The redox electrolyte contained 1,2-dimethyl-3-hexyl-imidazolium iodide (0.8 M) and iodine (40 mM) in acetonitrile. The radiant power is 100 mW/cm^2.

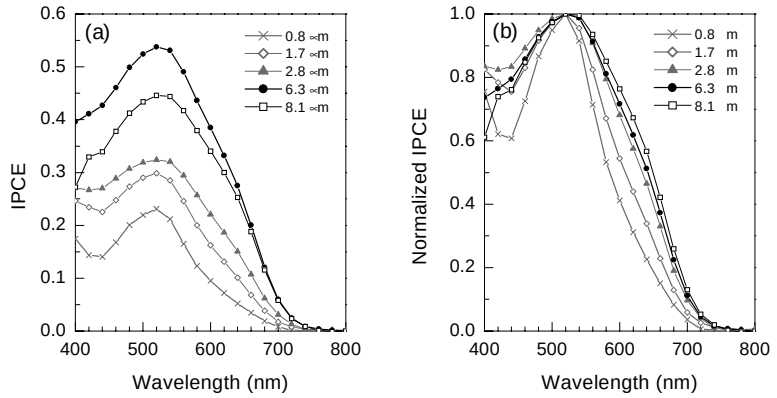

Fig. 7. Dependence of the (a) absolute and (b) normalized values of the IPCE on film thickness of dye-sensitized 10 mol.% Zn-modified nanocrystalline SnO_2 electrodes. The redox electrolyte contained 1,2-dimethyl-3-hexyl imidazolium iodide (0.8 M) and iodine (40 mM) in acetonitrile. No correction was made for reflection losses.

4. Conclusion

Surface-modified nanocrystalline SnO_2 films were prepared by treating a commercial Alfa Aesar SnO_2 colloid with zinc acetate. Acidification of the basic colloid solution induced the aggregation of the SnO_2 nanoparticles but zinc ions stabilize against individual nanoparticle growth. Upon modification with zinc acetate, coloration of the dye-adsorbed film became stronger, which however did not influence on J_{sc}. As increasing zinc concentration, V_{oc} and fill factor were significantly improved. In addition, zinc modification was found to utilize more red light. Within the present experiments, we found that 10 mol.% zinc-modified SnO_2 film with about 6 μm thickness showed best photovoltaic performance. For further improvement, modification of electrode, such as introducing light scattering particles to the zinc-doped SnO_2 film, is under study.

Acknowledgements

This work was supported by the Korean Ministry of Information and Communication (MIC) under contracts 2002-S-099 and 2002-S-013.

References

[1] B. O'Regan, M. Grätzel, Nature 353 (1991) 737.
[2] M. Grätzel, Nature 414 (2001) 338.
[3] M.K. Nazeeruddin, A. Kay, I. Rodicio, R. Humphry-Baker, E. Muller, P. Liska, N. Vlachopoulos, M. Grätzel, J. Am. Chem. Soc. 115 (1993) 6382.
[4] M.K. Nazeeruddin, P. Pechy, T. Renouard, S.M. Zakeeruddin, R. Humphry-Baker, P. Comte, P. Liska, L. Cevey, E. Costa, V. Shklover, L. Spiccia, G.B. Deacon, C.A. Bignozzi, M. Grätzel, J. Am. Chem. Soc. 123 (2001) 1613.
[5] I. Bedja, S. Hotchandani, P.V. Kamat, J. Phys Chem. 98 (1994) 4133.
[6] S. Ferrere, A. Zaban, B.A. Gregg, J. Phys. Chem. B 101 (1997) 4490.
[7] F. Fungo, L. Otero, E.N. Durantini, J.J. Silber, L.E. Sereno, J. Phys. Chem. B 104 (2000) 7644.
[8] S. Chappel, A. Zaban, Sol. Energy Mater. Sol. Cells 71 (2002) 141.
[9] H. Rensmo, K. Keis, H. Lindström, S. Södergren, A. Solbrand, A. Hagfeldt, S.-E. Lindquist, L.N. Wang, M. Muhammed, J. Phys. Chem. B 101 (1997) 2598.
[10] K. Keis, J. Lindgren, S.-E. Lindquist, A. Hagfeldt, Langmuir 16 (2000) 4688.
[11] B. O'Regan, D.T. Schwartz, S.M. Zakeeruddin, M. Gratzel, Adv. Mater. 12 (2000) 1263.
[12] K. Hara, T. Horiguchi, T. Kinoshita, K. Sayama, H. Sugihara, H. Arakawa, Sol. Energy Mater. Sol. Cells 64 (2000) 115.
[13] C. Bauer, G. Boschloo, E. Mukhtar, A. Hagfeldt, J. Phys. Chem. B 105 (2001) 5585.
[14] K. Keis, E. Magnusson, H. Lindström, S.-E. Lindquist, A. Hagfeldt, Sol. Energy Mater. Sol. Cells 73 (2002) 51.
[15] F. Lenzmann, J. Krueger, S. Burnside, K. Brooks, M. Gratzel, D. Gal, S. Ruhle, D. Cahen, J. Phys. Chem. B 105 (2001) 6347.
[16] G. Benkö, P. Myllyperkiö, J. Pan, A.P. Yartsev, V. Sundström, J. Am. Chem. Soc. 125 (2003) 1118.
[17] A.J. Nozik, R. Memming, J. Phys. Chem. 100 (1996) 13061.
[18] A. Hagfeldt, M. Grätzel, Chem. Rev. 95 (1995) 49.
[19] Y. Tachibana, K. Hara, S. Takano, K. Sayama, H. Arakawa, Chem. Phys. Lett. 364 (2002) 297.
[20] K. Tennakone, J. Bandara, P.K.M. Bandaranayake, G.R.A. Kumara, A. Konno, Jpn. J. Appl. Phys. 40 (2001) L732.
[21] N.-G. Park, M.G. Kang, K.M. Kim, K.S. Ryu, S.H. Chang, D.-K. Kim, J. van de Lagemaat, K. Bengkstein, A.J. Frank, submitted for publication.
[22] S. Chappel, S.-G. Chen, A. Zaban, Langmuir 18 (2002) 3336.
[23] A. Kay, M. Grätzel, Chem. Mater. 14 (2002) 2930.
[24] B.D. Cullity, Elements of X-Ray Diffraction, second ed., Addison-Wesley, Reading, MA, USA, 1977.
[25] S. Chappel, A. Zaban, Sol. Energy Mater. Sol. Cells 71 (2002) 141.
[26] G.A. Parks, Chem. Rev. 65 (1965) 117.
[27] A.P. Maciel, P.N. Lisboa-Filho, E.R. Leite, C.O. Paiva-Santos, W.H. Schreiner, Y. Maniette, E. Longo, J. Eur. Cer. Soc. 23 (2003) 707.
[28] E.R. Leite, A.P. Maciel, I.T. Weber, P.N. Lisboa-Filho, E. Longo, C.O. Paiva-Santos, A.V.C. Andrade, C.A. Paskocimas, Y. Maniette, W.H. Schreiner, Adv. Mater. 14 (2002) 905.
[29] Y. Diamant, S.G. Chen, O. Melamed, A. Zaban, J. Phys. Chem. B 107 (2003) 1977.